JP4.2 SURFACE HETEROGENEITY EFFECTS ON REGIONAL-SCALE FLUXES IN STABLE BOUNDARY LAYERS: AN LES STUDY

Rob Stoll * and Fernando Porté-Agel
Saint Anthony Falls Laboratory
University of Minnesota, Minneapolis, Minnesota

1. INTRODUCTION

Surface boundary conditions used in weather and climate models require the specification of turbulent fluxes of heat and momentum between the land surface and the atmosphere as a function of the grid-averaged velocity and temperature fields. Parameterizing these fluxes at the relevant regional scales has proven to be a challenge, especially under stable atmospheric stability conditions (Holtslag, 2005). This has led to numerous research efforts, mainly focused on homogeneous quasi-steady stable boundary layers (Beare et al., 2006).

The atmospheric boundary layer (ABL) is characterized by a wide range of length and time scales, which are highly dependent on the spatial distribution of land-surface properties such as temperature, aerodynamic roughness and soil moisture. The non-linear interaction between surface heterogeneities and atmospheric turbulence limits the applicability of similarity theories (e.g., the log-law), commonly used to model turbulent fluxes, and strictly is only applicable in homogeneous boundary layers. Under stable atmospheric conditions, the effect of stratification on local turbulence scales further complicates our ability to parameterize the effects of surface heterogeneity on ABL fluxes.

Previous numerical studies of surface heterogeneity have focused on either neutral (e.g., Glendening and Lin, 2002; Bou-Zeid et al., 2004; Stoll and Porté-Agel, 2006) or convective atmospheric stability conditions (e.g., Albertson et al., 2001; Patton et al., 2005). In contrast, the effect of surface heterogeneity under stable conditions has been explored mainly through experiments (e.g., Derbyshire, 1995; Mahrt and Vickers, 2005) and has yet to be studied with LES. Here we present some preliminary results from LES of the stable atmospheric boundary layer over heterogeneous surface boundary conditions.

This manuscript is organized as follows. First, a brief description of the LES code used in this study and the simulation setup used for the homogeneous and heterogeneous cases is given in section 2.1. In section 2.2, results are given for simulations with the scale-dependent Lagrangian dynamic model over heterogeneous surfaces with different length scales and amplitudes of heterogeneity.

2. NUMERICAL SIMULATIONS

2.1 *Case Description*

Our initial simulations of heterogeneous stable boundary layers focus on simple idealized surface patterns consisting of alternating patches with sharp streamwise changes in surface temperature. We use the LES code described by Stoll and Porté-Agel (2006). The code uses tuning-free Lagrangian dynamic subgrid-scale (SGS) models, designed to dynamically compute the SGS eddy viscosity and eddy diffusivity model coefficients based on the information contained in the resolved scales. In a recent study, these SGS models have been shown to dynamically adjust in a consistent manner to flow inhomogeneities associated with step changes in surface fluxes in neutral ABLs (Stoll and Porté-Agel 2006). This ability makes them ideally suited for the study of heterogeneous boundary layers.

Table 1: Mean boundary layer characteristics for the different surface types characterized by the temperature jump (in K) and the patch length (in m): homogeneous (Hom); 4 K, 400 m (Het4-400); 4 K, 200 m (Het4-200); 4 K, 100 m (Het4-100); 6 K, 400 m (Het6-400); 6 K, 200 m (Het6-200); and 6 K, 100 m (Het6-100).

case	δ (m)	u_* (m/s)	θ_* (K)	L (m)
Hom	178	0.260	-0.00140	127
Het4-400	193	0.271	-0.00111	172
Het4-200	194	0.273	-0.00110	177
Het4-100	195	0.275	-0.00109	181
Het6-400	207	0.279	-0.00083	252
Het6-200	210	0.283	-0.00081	264
Het6-100	211	0.286	-0.00081	269

The intermittent nature of the stable ABL renders it difficult to study experimentally or numerically (Mahrt, 1998; Beare et al., 2006). For this reason, we need an idealized and well studied stable boundary layer case as the basis for our heterogeneous simulations. This will make it easier to discern the effect of surface heterogeneity. The GEWEX (Global Energy and Water Cycle Experiment) ABL (GABLS) intercomparison study meets this criterion (Beare et al., 2006). To accommodate a larger range of surface heterogeneity scales some modifications to the GABLS case have been made. The domain size has been increased from 400 m to 800 m in the horizontal directions and from 400 m to 500 m in the vertical direction. Initial tests have been run with a resolution of 64 x 64 x 64 grid points in each direction. The surface temperature heterogeneity consists of alternating patches of two different surface temperatures with an average surface temperature over the entire domain equal to the one used in GABLS (initially 265 K). A total of seven simulations were performed: one homogeneous case, three cases with a temperature jump between patches of 6 K and three with a temperature jump between patches of 4 K. The temperature jumps are created by specifying different cooling rates for each patch while keeping the av-

*Corresponding author address: R. Stoll, Saint Anthony Falls, 2 3rd Avenue SE, Minneapolis, MN 55414, e-mail: stolli@msi.umn.edu

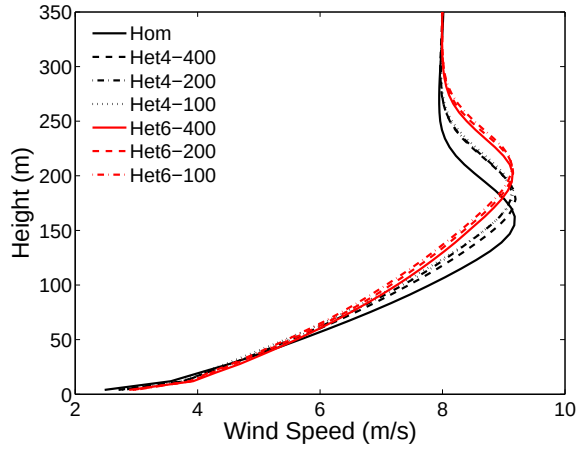

FIG. 1: Mean wind speed profile averaged over the last one hour of the simulation for homogeneous and heterogeneous stable boundary layer simulations. Legend abbreviations are the same as used in Table 1.

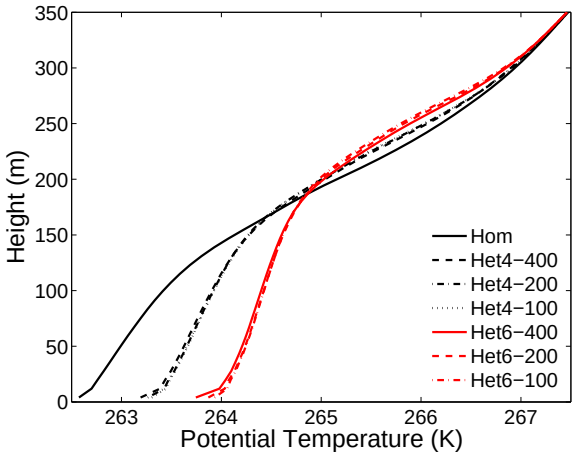

FIG. 2: Mean potential temperature averaged over the last one hour of the simulation for homogeneous and heterogeneous stable boundary layer simulations. Legend abbreviations are the same as used in Table 1.

erage cooling rate over the entire domain surface equal to that used in the GABLS study (0.25 K/hr). After eight hours, the cooling rate was returned to its average value and the simulation was continued for an additional four hours. This is required to ensure the simulations reach a quasi-steady state. The patch cooling rates were chosen to create the desired temperature differences after eight hours of simulation. The 4 K temperature jump simulations (hereafter referred to as Het4) were run with three different streamwise patch lengths, 400 m, 200 m and 100 m and the 6 K jump simulations (referred to as Het6) were run with three different patch lengths, 400 m, 200 m and 100 m. These patch lengths correspond to approximately 2 (400 m), 1 (200 m) and 1/2 (100 m) times the boundary layer height calculated at the end of the homogeneous run. A summary of the mean boundary layer characteristics (boundary layer height δ, friction velocity u_*, surface temperature scale $\theta_* = \langle w\theta \rangle_s u_*^{-1}$ where $\langle w\theta \rangle_s$ is the mean surface flux and Obukhov length $L = -u_*^3 T_o (\kappa g \langle w\theta \rangle_s)^{-1}$ and T_o is a reference temperature) are given in Table 1.

2.2 *Results*

As discussed in section 1, large scale models require the specification of surface fluxes of momentum and heat as a function of the grid-averaged velocity and temperature fields. In this section, we examine the effect of heterogeneous surface temperature distributions on surface flux parameterizations in stable atmospheric boundary layers. We present results from the series of simulations over idealized streamwise step changes in surface temperature outlined in section 2.1. The profiles depicted in this section all represent horizontal averages which are then averaged in time over the last 1 hour of each simulation.

The mean wind speed profiles from the six heterogeneous simulations and the homogeneous base case are shown in Figure 1. All of the profiles exhibit a nocturnal jet with a wind speed maximum slightly below the boundary layer heights given in Table 1. Above the boundary layer the wind speed approaches the geostrophic value in all the simulations. The homogeneous simulation closely matches the 12.5 m resolution simulations presented in Basu and Porté-Agel (2006) and the high resolution simulations presented in Beare et al. (2006). All of the heterogeneous simulations show a clear deviation from the homogeneous case. The wind speed maxima occur at elevated levels with respect to the homogeneous case. Furthermore, the wind maxima in the Het6 simulations occur at higher levels than in the Het4 simulations. This increase in wind maxima height corresponds to the increases in boundary layer height reported for the different simulations in Table 1. Notice that the strength of the surface temperature jump appears to have a stronger effect on the wind speed profile than the patch length. Within the lowest 50 m of the simulation domain, the profiles show only minimal deviation from the homogeneous case.

Figure 2 shows the mean potential temperature profiles for all the simulations. Similar to the wind speed profile, the homogeneous temperature profile closely follows the simulation results from Basu and Porté-Agel (2006) and Beare et al. (2006). All of the profiles show positive curvature above the surface inversion as implied by Nieuwstadt's theoretical model (Basu and Porté-Agel, 2006). These profiles show a similar systematic dependence on surface heterogeneity to those shown in Figure 1. The Het4 and Het6 simulations all show an increased potential temperature throughout the entire boundary with respect to the homogeneous case. This pattern agrees with the decreased (in magnitude) heat flux values and increased Obukhov lengths in Table 1. Neither set of cases shows significant dependence on patch length scale for the range of length scales tested here.

To further explore the effect of heterogeneous surface temperature on the stable boundary layer we plot the non-dimensional shear Φ_M as a function of the stability parameter z/L in the surface layer. Φ_M is defined as

$$\Phi_M = \frac{\kappa z}{u_*} \sqrt{\left(\frac{\partial \langle u \rangle}{\partial z}\right)^2 + \left(\frac{\partial \langle v \rangle}{\partial z}\right)^2} \qquad (1)$$

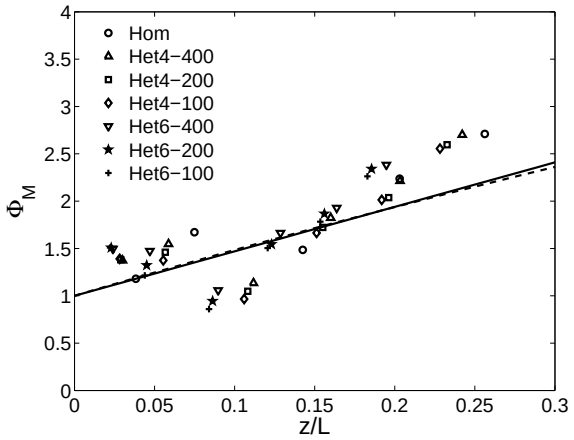

FIG. 3: Non-dimensional velocity gradient as a function of z/L in the lowest 50 m of the domain. The solid line and dashed lines correspond to the formulations proposed by Businger et al. (1971) and Beljaars and Holtslag (1991), respectively.

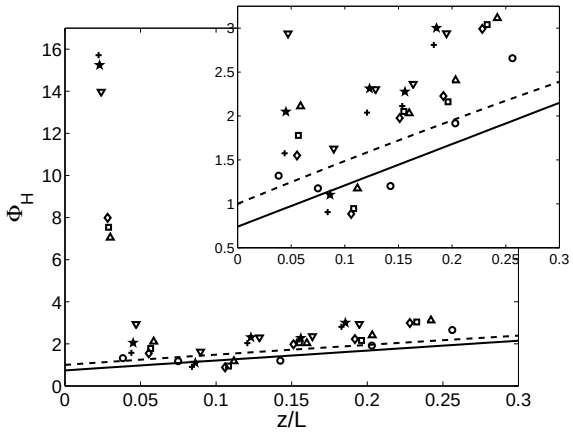

FIG. 4: Non-dimensional potential temperature gradient as a function of z/L in the lowest 50 m of the domain. Graph symbols are the same as Figure 3 and the solid line and the dashed line correspond to the formulations proposed by Businger et al. (1971) and Beljaars and Holtslag (1991), respectively. The insert shows the plot without the lowest z/L value.

in which κ =0.4 is the von Karman constant and $\langle u \rangle$ and $\langle v \rangle$ are the mean velocity components in the streamwise and spanwise directions, respectively. Most large scale models use the integral of Φ_M (i.e. the modified log profile) to calculate the surface shear stress (Beljaars and Holtslag, 1991; Mahrt, 1996).

In Figure 3 no clear signature of the heterogeneous surface temperature can be deduced. This agrees with the mean wind speed profiles in the surface layer shown in Figure 1. The lack of dependence of the non-dimensional shear on heterogeneous surface temperature distributions is an indication that while the heterogeneity results in an increased boundary layer height, it does not change the functional relationship between the average velocity profiles and momentum fluxes in the surface layer. Therefore, traditional similarity type momentum flux parameterizations should be able to adequately describe the cases presented here.

The non-dimension temperature gradient Φ_H is presented in Figure 4 as a function of the stability parameter z/L. Φ_H is defined as

$$\Phi_H = \frac{\kappa z}{\theta_*} \frac{\partial \langle \theta \rangle}{\partial z} \tag{2}$$

where $\langle \theta \rangle$ is the potential temperature averaged over horizontal planes and in time. The non-dimensional temperature gradient has a more distinct dependence on heterogeneous surface temperature than the non-dimensional shear. The cases with the largest temperature jumps deviate the most from the homogeneous case. In contrast to the mean temperature profiles, there appears to be some dependence on patch size, with increasing patch size resulting in larger gradients. This effect is pronounced enough that the Het4-400 case gradients consistently exceed those from the Het6-100 case. The overall effect of temperature jump strength and patch size results in large deviations from the homogeneous case at the lowest level for all of the cases. This carries into the lowest z/L values where gradients are about twice the homogeneous ones or more. These results indicate that proper estimation of surface heat fluxes for the heterogeneous cases presented here would require a correction to Φ_H or a different parameterization methodology.

3. SUMMARY

Large eddy simulations of a quasi-steady stable atmospheric boundary layer are performed over various idealized surface temperature heterogeneity patterns. The heterogeneity consists of streamwise step changes in surface temperature with varying patch lengths. Mean boundary layer characteristics show consistent trends with surface heterogeneity for temperature statistics (surface flux, mean potential temperature and non-dimensional temperature gradient) which show greater sensitivity than the corresponding momentum statistics. For example, the mean potential temperature in the boundary layer increases for all of the temperature jumps. Likewise, the non-dimensional temperature gradient strongly deviates from the homogeneous case for all of the Het6 simulations and the Het4 simulations. For both Het4 and Het6 cases, even the smallest patch size shows important deviations from the homogeneous case. This can be explained by the relatively small size of the eddies in the stable boundary layer simulations (Derbyshire, 1995; Mahrt, 1998). Note this is in contrast to neutral and convective boundary layers where eddies on the order of the boundary layer height induce enhanced mixing, minimizing the effect of heterogeneities smaller than the boundary layer height (Mahrt, 2000).

Our future work on heterogeneous stable boundary layers will include studying numerical simulation issues such as the sensitivity of our results to grid resolution and the specification of the LES surface boundary conditions. We will also examine the detailed structure of the internal boundary layers created by the surface temperature jumps.

ACKNOWLEDGMENTS

The authors gratefully acknowledge funding from NSF (grants EAR-0094200 and EAR-0537856) and NASA

(grants NAG5-11801 and NNG06GE256). R.S. was supported by a NASA Earth Systems Sciences fellowship (training grant NNG04GR23H). Computing resources were provided by the University of Minnesota Supercomputing Institute.

References

Albertson, JD, Kustas, WP, and Scanlon, TM. 2001, Large-eddy simulation over heterogeneous terrain with remotely sensed land surface conditions. *Water Resources Res.*, **37(7)**: 1939-1953.

Basu, S, and Porté-Agel, F. 2006, Large-eddy simulation of stably stratified atmospheric boundary layer turbulence: a scale-dependent dynamic modeling approach. *J. Atmos. Sci.*, in press.

Beare, RJ, MacVean, MK, Holtslag, AAM, Cuxart, J, Esau, I, Golaz, JC, Jimenez, MA, Khairoutdinov, M, Kosovic, B, Lewellen, D, Lund, TS, Lundquist, JK, McCabe, A, Moene, AF, Noh, Y, Raasch, S, and Sullivan, PP. 2006, An intercomparison of large-eddy simulations of the stable boundary layer. *Boundary Layer Meteor.*, in press.

Beljaars, ACM, and Holtslag, AAM. 1991, Flux parameterizations over land surfaces for atmospheric models. *J. Appl. Meteorol.*, **30**: 327-341.

Bou-Zeid, E, Meneveau, C, and Parlange, MB. 2004, Large-eddy simulation of neutral atmospheric boundary layer flow over heterogeneous surfaces: blending height and effective surface roughness. *Water Resources Res.*, **40**: 1-18.

Businger, JA, Wyngaard, JC, Izumi, Y, and Bradley, EF. 1971, Flux-profile relationships in the atmospheric surface layer. *J. Atmos. Sci.*, **28**: 181-189.

Derbyshire, SH. 1995, Stable boundary layers: observations, models and variability part I: modelling and measurements. *Boundary Layer Meteor.*, **74**: 19-54.

Glendening, JW, and Lin, CL. 2002, Large eddy simulation of internal boundary layers created by a change in surface roughness. *J. Atmos. Sci.*, **59**: 1697-1711.

Holtslag, B. 2005, Stable boundary layers and land surface climate: results from the GEWEX atmospheric boundary layer study. *iLEAPS Newsletter*, **Nov.**: 18-19.

Mahrt, L. 1996, The bulk aerodynamic formulation over heterogeneous surfaces. *Boundary Layer Meteor.*, **78**: 87-119.

Mahrt, L. 1998, Stratified atmospheric boundary layers and the breakdown of models. *Theoret. Comput. Fluid Dynamics*, **11**: 263-279.

Mahrt, L. 2000, Surface heterogeneity and vertical structure of the boundary layer. *Boundary Layer Meteor.*, **96**: 33-62.

Mahrt, L, and Vickers, D. 2005, Boundary-layer adjustment over small-scale changes of surface heat flux. *Boundary Layer Meteor.*, **116**: 313-330.

Patton, EG, Sullivan, PP, and Moeng, CH. 2005, The influence of idealized heterogeneity on wet and dry planetary boundary layers coupled to the land surface. *J. Atmos. Sci.*, **62**: 2078-2097.

Stoll, R, and Porté-Agel, F. 2006, Dynamic subgrid models for momentum and scalar fluxes in large-eddy simulations of neutrally stratified atmospheric boundary layers over heterogeneous terrain. *Water Resources Res.*, 2006; **42(1)**: W01410.